Norsk Regnesentral
ANVENDT DATAFORSKNING

Rapport/Report

Tittel/Title:
Model-based estimation of transcript concentrations from spotted microarray data

Dato/Date: May
År/Year: 2004
ISBN: 82-539-0507-6
Publikasjonsnr.: 999
Publication no.: 999

Forfatter/Author:
Arnoldo Frigessi, Mark A. van de Wiel, Marit Holden, Ingrid K. Glad, Heidi Lyng

Sammendrag/Abstract:
Much data from spotted microarrays remain unused because obtained with different protocols, platforms or designs, making comparisons across experiments impossible. We have developed a model-based method, which provides absolute transcript levels. Transcript levels are universal, and can be included in further analyses with similar estimates obtained with different techniques in other laboratories. It is a first step both towards genuine meta-analyses, including comparisons across different organisms, and the building of data bases of transcript levels in cells. Our method is based on statistical modelling incorporating all available information about the experiment, from target preparation to image analysis, coherently propagating uncertainties from data to estimates. It requires some genes spotted in replicates, their number being related to the levels of experimental factors included in the model, but not to the number of spotted genes. No uncertainty in the estimates caused by decimated data sets, indirect comparisons, normalisation or imputation of missing values, is introduced, leading to a far more precise analysis of microarray data than provided by conventional methods. Using a flexible Bayesian technique we estimate the highly multivariate joint posterior distribution of all transcripts, which enables extended exploitation of the data. In the present work we show that the estimated transcript concentrations are accurate and reproducible, and demonstrate improved statistical tools for selecting genes based on their concentration in highly unbalanced experimental settings.

Emneord/Keywords: mRNA transcript concentrations; spotted microarray data; Bayesian hierarchical models; MCMC

Tilgjengelighet/Availability: Open

Prosjektnr./Project no.: 220150, 220091, 830105

Satsningsfelt/Research field: Bioinformatics

Antall sider/No. of pages: 40

Norsk Regnesentral / Norwegian Computing Center
Gaustadalléen 23, Postboks 114 Blindern, 0314 Oslo, Norway
Telefon 22 85 25 00, telefax 22 69 76 60

Model-based estimation of transcript concentrations from spotted microarray data.

Arnoldo Frigessi[1,2], Mark A. van de Wiel[2,3], Marit Holden[2], Ingrid K. Glad[4] and Heidi Lyng[5]

1. Department of Statistics, Institute of Basic Medical Sciences, University of Oslo, Oslo, P.O. Box 1122 Blindern, 0317 Oslo, Norway

2. Norwegian Computing Center, P.O. Box 114 Blindern, 0314 Oslo, Norway

3. Present address: Department of Mathematics and Computer Science, Technische Universiteit Eindhoven, P.O. Box 513, 5600 MB Eindhoven, The Netherlands

4. Department of Mathematics, University of Oslo, P.O. Box 1053 Blindern, 0316 Oslo, Norway

5. Department of Biophysics, The Norwegian Radium Hospital, Montebello, 0310 Oslo, Norway

Correspondence should be addressed to A.F. (frigessi@medisin.uio.no, telephone: +4722851004, fax: +4722851313).

Classification. Major: Biological Sciences; Minor: Genetics, Statistics.

Manuscript information:

Number of text pages (including references and figure legends): ;

Number of figures: ;

Number of words in the abstract: .

Number of characters in the paper: .

Abbreviation footnote: MCMC - Markov chain Monte Carlo

Data deposition footnote: The data and the software used in this paper can be downloaded here: http://www.nr.no/pages/samba/area_emr_smbi_transcount.

Date of submission: - this is pnas version 4

Abstract

Much data from spotted microarrays remain unused because obtained with different protocols, platforms or designs, making comparisons across experiments impossible. We have developed a model-based method, which provides absolute transcript levels. Transcript levels are universal, and can be included in further analyses with similar estimates obtained with different techniques in other laboratories. It is a first step both towards genuine meta-analyses, including comparisons across different organisms, and the building of data bases of transcript levels in cells. Our method is based on statistical modelling incorporating all available information about the experiment, from target preparation to image analysis, coherently propagating uncertainties from data to estimates. It requires some genes spotted in replicates, their number being related to the levels of experimental factors included in the model, but not to the number of spotted genes. No uncertainty in the estimates caused by decimated data sets, indirect comparisons, normalisation or imputation of missing values, is introduced, leading to a far more precise analysis of microarray data than provided by conventional methods. Using a flexible Bayesian technique we estimate the highly multivariate joint posterior distribution of all transcripts, which enables extended exploitation of the data. In the present work we show that the estimated transcript concentrations are accurate and reproducible, and demonstrate improved statistical tools for selecting genes based on their concentration in highly unbalanced experimental settings.

Efficient production of spotted glass-slide arrays has made the microarray technology to a widespread technique, and improved methods to extract and summarise useful information are needed (1; 2; 3). The basic elements are normalised intensity ratios between two biological samples, hybridised together in a single experiment. To allow comparative analysis, the experimental design is transitive, often with a loop or a common reference sample (4; 5; 6). Such design requirements and the need for stable references impose serious constraints on data use. Methods assessing absolute rather than relative transcript measures would enable integration of data from different sources in global analyses, independent on experimental protocol, design and microarray platform (cDNA and oligonucleotides). Such methods are a principle goal if durable compendia of gene expressions in terms of transcripts per cell, analogous to DNA sequence database information, are to be achieved (1; 7).

Extraction of absolute transcript levels from spotted microarray data is complicated due to significant experimental variation and noise originating in the production and hybridisation processes (2; 3; 4). Normalised intensity ratios reduce the influence of systematic effects in the data, though biological information might be lost (8; 9). Model-based analysis opens for use of experimental and biological information to increase the accuracy of calculated transcript levels. Linear statistical models have proven successful for identification of differentially expressed genes but absolute transcript levels cannot be obtained (9; 10; 11).

We have developed a new model based on a radically different principle that enables estimation of absolute transcript levels, thus allowing extended exploitation of microarray data. Experimental information associated with array-, cDNA synthesis-, hybridisation-, and scanning characteristics was incorporated. The model follows the different steps of the microarray experiment. Our method also constitutes an improved analysis tool. We compute the joint posterior distributions of either the absolute or relative transcript levels and reveal dependencies between genes, both within and between individual samples. Uncertainties from sample preparation to imaging have been coherently propagated in a global statistical approach.

Our method was validated on a dataset with known mRNA concentrations. On a second dataset we demonstrate Bayesian analysis. We show that significant results can be obtained from data with limited repetitions. The model can handle experiments based on amplified as well as nonamplified material. The results are based on spotted cDNA microarrays, which feature particularly large experimental variation, but our model can directly be applied to spotted oligoarrays.

Methods

Principles. The idea is to follow conceptually the mRNA molecules through the microarray experiment, from cDNA synthesis to hybridisation and subsequent washing (Fig. 1). We modelled the process as a stepwise selection, where each molecule had a certain probability of being kept in the experiment. This probability depended on known experimental covariates, like mRNA purity, array, pen, gene, and probe identification, replication, length and quantity. We treated scanning and image analysis as an integral part of the experiment and used associated covariates, such as dye, scanner setting and spot size. Also a scanner and a hybridisation-technique specific characteristic were included: The scanner amplification factor was needed to account for differences in the intensity response among scanner types; the hybridisation factor identified the absolute scale of the estimates. Both were determined in two off-line calibration experiments.

Basic data are the average fluorescence intensities of each spot and their standard deviations, for each experiment. No transformation nor normalisation should be done. Non-transitive data sets are allowed as long as the design includes at least one loop, like a self-self or dye-swap hybridisation. Some genes must be spotted at least in duplicates, their number being independent on the number of genes in the analysis, but related to identifiability of pen effects. In our case, 50 duplicates were enough to identify effects of the six pens used. Experiments with amplified material are handled like those with nonamplified one, but estimates are transformed back to original scale (11).

We performed Bayesian inference and calculated the posterior joint distribution of all unknown parameters using MCMC (12). We estimated the number of transcripts for each gene in each sample together with their uncertainty, described by 95% credibility intervals. The posterior joint distribution reflects biological dependency between the number of transcripts, inferred from the data, which cannot be attributed to the experiment. The posterior joint distribution is needed to compute interesting probabilities, such as the probability for a transcript of being among those with highest (or lowest) concentrations.

Covariates. The steps of the microarray experiment were modelled as a binomial selection process, incorporating covariates associated with cDNA synthesis, dye labelling, purification, hybridisation, washing (Fig. 1 and Supporting Methods 1). The corresponding covariates were array, pen, gene, probe replication (RID), probe identification (PID), probe length, and probe quantity. Replicated genes had PID and RID effects: PID accounted for different probes, and RID for replications of equal probe. The number of base pairs in the probe sequence was used as probe length. A test slide of each printing series was stained for single stranded DNA by

use of SYBR green II (Molecular Probes). The mean spot fluorescence intensities were used as measures of probe quantity. Probe quantity was included since hybridization efficiency of high density probes may be reduced (13).

Covariates associated with scanning were dye, PMT voltage and the scanner amplification factor. The dye covariate represented the dye effect in both labelling and scanning. The amplification factor is a measure of the increase in intensity per unit of increase in PMT voltage. The factor was determined once for each dye and scanner as the slope in log-linear plots of intensity versus PMT voltage (14). A covariates associated with image analysis is the hybridisation factor, used to scale the estimated values to the true number of transcripts. It was determined using two control samples with transcripts at known concentrations, with weighted linear regression of estimates versus true values. Under ordinary stable experimental settings it is sufficient to determine the factor once for each hybridisation method, for example for manual hybridisation and for each type of hybridisation machine.

Statistical Methods. Consider several biological samples. The known quantity of material for sample t on array a is denoted as $q^{t,a}$, for example the weight of mRNA after amplification. For each gene g, let K_g^t denote the unknown number of transcripts per weight unit present in sample t (Fig. 1). Let $L_{j,s}^{t,a}$ be the measured intensity for sample t in pixel j in spot s on array a. The hierarchical, non-linear model that relates these data to the number of transcripts, consists of three layers: (i) a model for the selection process, describing the proportion of target molecules (from the original $q^{t,a} \cdot K_g^t$) that have survived the several steps of the experiment until washing of the hybridised slides; (ii) a model for the scanning process of the hybridised slides; (iii) a model for measurement and residual errors.

In (i), the $q^{t,a} \cdot K_g^t$ molecules undergo a series of processes from cDNA synthesis to hybridisation and washing (Fig. 1). Let n_s^a be the number of pixels in spot s on array a and n_g^a the total number of pixels in all spots related to gene g on array a. After successful cDNA synthesis, labelling and purification, a proportion $c \cdot n_g^a$ of the $q^{t,a} \cdot K_g^t$ molecules candidates to reach the correct spots for hybridisation. Here c is the hybridisation factor per pixel. Each of these $c \cdot n_s^a \cdot q^{t,a} \cdot K_g^t$ molecules has a success probability $p_s^{t,a}$ to hybridise and to remain fixed after subsequent washing, independently of other molecules. This independency corresponds to the usual *probe in excess* assumption. As discussed in Supporting Methods 1, $p_s^{t,a}$ also accounts for successful cDNA synthesis, dye labelling and purification and it depends on biological and experimental conditions described by covariates. Let $H_s^{t,a}$ be the unknown number of molecules in sample t that succeeds in hybridising on spot s on array a, resists

subsequent washing, thus being available for imaging. Then

$$H_s^{t,a} \sim \text{Binomial}(c \cdot n_s^a \cdot q^{t,a} \cdot K_g^t,\, p_s^{t,a}),$$

where g is the gene spotted in spot s on array a and

$$\begin{aligned} p_s^{t,a} &= \max[1, \exp\{\beta_0 + \beta_e + \beta_a + \beta_p + \beta_g + \beta_{\text{RID}} + \beta_{\text{PID}} \\ &\quad + \beta_l \cdot [\text{probe length}] + \beta_q \cdot [\text{probe quantity}] + \beta_m \cdot [\text{purity}_t]\}]. \end{aligned} \tag{1}$$

The β's represent effects of the various covariates for spot s on array a (β_a array, β_p pen, β_g gene, β_{PID} probe identification, β_{RID} probe replication), [probe length] is the number of base pairs of the probe in spot s, [probe quantity] is the SYBR green intensity, $[\text{purity}_t]$ is the purity of sample t. $\exp(\beta_0)$ is the global baseline selection probability. When non-transitive data sets are analysed jointly, an effect β_e is required for each transitive subset. Identifiability is assured, see Supporting Methods 2.

In (ii), the expected scanned intensity on spot s, array a, is modelled as

$$\mu_s^{t,a} = 2^{f_{\text{dye}} \cdot \text{PMT}^{t,a}} H_s^{t,a} \alpha_{\text{dye}}, \tag{2}$$

where $\text{PMT}^{t,a}$ is the PMT-voltage used during scanning of sample t on array a, f_{Cy3} or f_{Cy5} are the known scanner amplification factors, while α_{Cy3} and α_{Cy5} are unknown chemical and optical dye effects.

In (iii), we assume for the pixel-wise intensity measurement $L_{j,s}^{t,a}$

$$L_{j,s}^{t,a} = \frac{\mu_s^{t,a}}{n_s^a} + \varepsilon_{j,s}^{t,a}, \tag{3}$$

where $\varepsilon_{j,s}^{t,a}$ is a normally distributed error term with a spot varying variance $(\sigma_s^{t,a})^2$. By conditional independence of the pixel-wise intensities, only the spot-wise mean intensity is required in computations. $\varepsilon_{j,s}^{t,a}$ is estimated directly from the intensities as their sample variance in each spot. Background correction can be included at this level, but was not in our examples.

In the statistical analysis of several arrays and samples, many of the unknown parameters are shared, like array, dye, pen, gene and probe related effects; all data involving sample t contribute information on the unknowns K_g^t. To assure statistical identifiability, some genes must be spotted at least in duplicate. The number of replicated genes is independent on the total number of spotted genes, since replicates are used to estimate the common parameters. The whole data set must include at least one loop, i.e. a self-self array or a dye swap or a longer chain, necessary to identify the relative dye effect $\alpha_{Cy3}/\alpha_{Cy5}$. Beyond this, we do not require a transitive design. To facilitate estimation, the model is reparametrised, so that the baseline β_0, β_e, β_g, β_m and α_{Cy5} are estimated only on the basis of the variances in the

Binomials. Data relative to non-duplicated genes and samples hybridised only once are not used to estimate variances (Supporting Methods 2). MCMC was implemented to compute the joint and marginal posterior distributions of unknowns of interest (Supporting Methods 3). The joint distribution describes dependencies between unknowns, for example between K_g^t's for various genes and samples. A priori nothing is assumed on the number of transcripts. The model introduces dependency, through shared experimental factors, so that the quantities $H_s^{t,a}$ are dependent. Dependencies in the data are then attributed backwards in part to this experimental dynamics, and to the posterior joint distribution of the K_g^t's. Estimates of parameters are marginal posterior modes with 95% symmetric credibility intervals.

Materials

Human cDNA microarray slides were printed with 32 pens. Probe length ranged from 525 to more than 2000 base pairs. For validation of our method, 17 DNA control samples were printed in equal amount on six subarrays. We used two control samples, each containing 17 different mRNA sequences, pre-mixed at specific concentrations. 0.5 μl of each sample was used, corresponding to a number of transcripts in the range of $5.8 \times 10^5 - 5.8 \times 10^9$. The concentration ratios achieved when hybridising the two samples together were 1:1, 1:3, 3:1, 1:10, and 10:1 at high and low level concentrations. The labelled samples were hybridized together in a dye-swap design. In a second experiment, two tumour biopsies (A, B) and a reference sample (Ref) of total RNA (Stratagene) were used. The biopsies were from two different locations in a human cervical tumour. Biopsy B was divided into two pieces (B1, B2). Total RNA was isolated (50 to 60 μg) and used to produce labelled cDNA. The samples were hybridized in a loop design (Table 1). RNA purity was optimal and equal for all samples in our experiments and was therefore not used. The slides were imaged at a resolution of 10 μm using an Agilent G2565BA scanner (Agilent Technologies) for slides with control samples and a ScanArray4000 scanner (GSI Lumonics) for slides with biopsies and reference. A laser power of 100% was used. The PMT voltage was adjusted for the red and green channel individually (14). See Supporting Materials for details.

Results

Validation of the methodology. To validate our method we used dye-swap experiments with control samples at known concentrations. The spot intensities covered the whole detection range, from near background values to saturation. There was a good accordance between the

true and estimated number of mRNA molecules (Fig. 2A), but the lowest numbers (below 10^6) were overestimated, consistent with other studies (15; 16; 17), possibly because low intensity spots had more noise. Background correction improved estimates (data not shown). The uncertainty of our estimates increased for the most abundant molecules with numbers above 10^9. The hybridisation factor was 0.001. Ratios between numbers of molecules per gene in the two samples were also well estimated (Supporting Figure 7).

We analysed a second, independent experiment, with identical design and protocol (Fig. 2B) using the hybridisation factor 0.001. There was again good accordance between true and estimated values with a systematic underestimation of $\log_{10}$-concentrations by 0.1, small enough not to influence the estimated values significantly, since $\log_{10}$-concentrations were in the range 6 to 10. The hybridisation factor based on the second experiment was 0.0008. The difference between the two hybridisation factors was small.

To illustrate meta-analysis, two non-transitive dye-swap experiments were analysed: samples A and B for the first experiment (Fig. 2A) and samples C and D for the second (Fig. 2B). Here, $A = C, B = D$ and each data set was analysed separately, with hybridisation factor 0.001; the model had no knowledge that samples in the first experiment were repeated in the second one. Since the estimates in Fig. 2A and B were almost equal, we concluded that meta-analysis was successful. The estimated numbers of mRNA molecules for each sample are directly comparable and can be used in further analysis.

Tools for data analysis. In the second experiment, four arrays were hybridised in a loop design with three samples (A, B1, B2) from a human cervical tumour and a reference sample (Ref) (Table 1). It is not clear how to compare optimally the measured intensity ratios with standard methods (4). We considered 100 genes on 158 spots of each array; 27 genes were duplicated with different probe sequences, 31 genes were duplicated with identical probe sequences, 42 genes were singles. Five different pens were used. This design is unbalanced. Although only a limited number of genes were considered here for illustrative purposes, our method can be equally used for larger data sets of thousands of genes and many samples. To provide concentrations, the estimated numbers of transcripts were related to the known weight of the total RNA.

Estimated concentrations for individual genes were reliable, as pairwise scatterplots (Supporting Figure 8), and correlations show (Supporting Table 3). Results were consistent with A, B1 and B2 originating from the same tumour and B1 and B2 originating from the same location within the tumour. We investigated reproducibility of our result by splitting the data into two sets of two arrays each, (Ref-B1, B1-B2) and (B2-A, A-Ref). We analysed these separately, pretending samples were not shared. The estimated numbers of transcripts were

very similar for the identical samples, B2 and Ref, showing high reproducibility in our results (Fig. 3). This similarity supports our claim that estimated numbers of transcripts of different samples can be compared and combined, also when originating from separate experimental schemes, with no transitive design. For example we can compare directly the transcript concentrations in sample A and B1 though the design did not link them transitively.

In experiments based on total RNA it can be investigated if the proportion of mRNA in total RNA is equal for all samples by comparing the sum of all estimated numbers of transcripts in each sample. For the present data with 100 genes, we obtained the sum $5.97 \cdot 10^7$ for sample B1, $5.96 \cdot 10^7$ for B2, $6.17 \cdot 10^7$ for A and $4.49 \cdot 10^7$ for the reference. The similarity of these values for the three tumour samples is consistent with these originating from the same tissue.

We estimated experimental and probe related factors, describing to what extend they influence selection probabilities (Supporting Table 4). In the second experiment, the four array effects β_a were $-0.54, -0.04, 0.18, 0.40$. This indicated differences in hybridisation efficiency between the four arrays due to non-modelled factors influencing the entire arrays, for example during array production (humidity, temperature). The probe length effect β_l was -0.17, as important as the array effect. The negative sign means that probes with short length have a higher probability to retain molecules for imaging, after hybridisation and washing. Estimated effects can be further used to improve protocols, identifing sources of experimental variation.

Many studies investigate the characteristic gene expressions of a population with a certain trait, using a set of biological samples. We can estimate the characteristic mRNA concentration for each gene of such a population. In the context of the present data set, we first computed the mean of the estimated concentrations of the three tumour samples for each of the 100 genes. The probability densities of mean concentration were often non-normal and skewed (Supporting Figure 9). Second, we computed for each gene the probability that its mean concentration was among the n highest (Fig. 4). This involves a 100-dimensional integration of the posterior joint distribution performed with MCMC. The steepness of the curve describes the level of concentration of a gene compared to others.

We show two probabilistic gene selection methods: in the first, ranking occurs on the basis of absolute concentrations; the second method requires a threshold on concentrations or on folds of concentration ratios.

First, we evaluated the probability that any single gene in turn had a mean concentration among the highest (or lowest) 10. We then ranked all genes according to this probability (Fig. 5). Low mRNA concentrations are associated with more uncertainty than high ones, resulting in less candidate genes with low concentration (15). This ranking is independent of any chosen reference sample.

For the second selection method, we considered estimated ratios of mean concentrations in the tumour vs. reference. Suppose we ordered the genes according to a certain criterion, but we only wanted to select those genes that were with high probability at least k-fold expressed. Using the joint distribution, we require that all genes in the selected set are at least k-fold expressed, jointly. Alternatively, we can relax our request and allow m errors (falsely k-fold expressed). Hence, we computed the probability that all but m genes were at least k-fold expressed, and ordered the genes according to the probability that their concentration ratio was among the ten highest or lowest (Fig. 6). Seven genes would be selected, when allowing no errors ($m = 0$) and requiring 2-fold expression ($k = 2$) with 95% joint probability. Alternatively, one may fix the probability (to say 0.95) and the accepted number of errors m and then study the number of selected genes as function of the fold k (Supporting Figure 10). These plots help choosing candidate genes. The first selection method is useful for concentrations, for which there is no natural cut-off value and we use a probability to rank genes. When natural thresholds are available, like folds of ratios, the second method is useful, since it explicitly controls the joint probability level.

Discussion

We have proposed a new method for estimating precisely the transcript level of individual genes from spotted microarray intensity data and obtained the joint distribution of absolute (or relative) transcript levels, which portraits the dependencies between absolute (or relative) mRNA concentrations. Once the transcript levels have been estimated, radically new analyses are possible, including within sample comparison, merging of data sets with a design lacking transitivity or based on amplified and non-amplified starting materials, cross-platform and cross-species comparisons and more general meta-analysis. This may open for novel approaches in the study of several biological processes, including signal transduction pathways.

Our method is based on four main ideas: we incorporate an extended number of covariates compared to other models (2); we treat unequal number of replicates per gene; we use the binomial process, which better depicts experimental dynamics and allows for estimation of the critical parameters β_0, β_g, and $\alpha_{Cy3/Cy5}$; we avoid normalisation and imputation of missing values and build a bottom-to-top coherent stochastic model, fully propagating uncertainty. The accuracy of our estimates was better than in Dudley et al. (16), especially at medium and low concentrations, and in fact comparable to that achieved from methods based on in situ synthesized arrays (15; 17), despite this technology uses standardised manufacturing and hybridisation, so that probe specific biases are highly reproducible and predictable (18).

There are limitations of our methodology. Cross-hybridisation and unspecific binding are not taken into account, and possible splice-variants for some of the genes are not considered. Currently, no analysis tools for microarray data are addressing these aspects. Other covariates could easily be included in our model when available, such as target length and labelling efficiency, probably leading to higher accuracy in the estimates. The MCMC algorithm converges slowly. Results can require up to a few days of computation time.

Few methods estimating absolute transcript levels from spotted microarray data have been developed so far. The method by Dudley et al. (16) requires hybridisation of each sample with a reference of known concentration, imposing serious restrictions. Other methods rely on calibration of each array with additional techniques, such as serial analysis of gene expression (SAGE) (19). The present method is the first quantifying absolute transcript levels from spotted microarray data without the need for calibration of each sample individually. Moreover, it can be used to estimate absolute concentrations from one or multi-color experiments, and it can directly be applied to data from spotted oligoarrays, using base composition of the probes as covariates rather than the probe length. The hierarchical structure of our model enables integration of biological information about the samples, such as patient survival data, and known dependencies between genes, in a coherent Bayesian setting. If the mRNA weight is not available and significant variability in the proportion of mRNA in total RNA is suspected, or if the hybridisation factor is not available, it is possible to scale each sample so that the sum of estimated transcripts are equal. Comparison of such scaled concentrations is still possible between samples, but the interpretation as absolute concentrations is lost.

We estimated concentration ratios more accurately than concentrations themselves, because the uncertainty in the intercept β_0 influences only the absolute numbers and not the ratios. We obtain ratios of concentrations, while usually intensity ratios are compared, whose fold changes can be misleading since they might not correspond to fold changes of actual transcript concentrations (9). In addition our method provides for the first time highly reliable ratios between concentrations of different genes in the same sample.

With our method few constraints are imposed on the experimental design and no normalisation and imputation of missing values is needed. The common reference design requires stable reference samples, uselessly measured many times (6). A balanced design is required to apply linear mixed effect models in practice (9). Thus our method opens for new possibilities of meta-analyses (7). Such analyses are currently built on top of statistical tests to detect differential expressions (20; 21). Since the result of these tests may depend on experimental protocol and microarray platform, bias may lead to wrong conclusions. With our method, data from different studies can be combined at the basic level of transcript concentrations

or concentration ratios, regardless of whether studies use amplified or non-amplified starting material, cDNA or oligonucleotide platforms. Available data can therefore be re-used in new investigations, leading to a better exploitation of the data and more precise results.

In our model, normalisation is performed unsupervised, as in ANOVA based methods (9); we incorporate explicitly more sources of variability, including scanning. Current normalisation methods are often platform dependent and based on hypothesis on the gene expressions difficult to test. Misuse of normalisation is rather common in practice (22). The need for balanced designs often leads to discarding genes or requires imputation of missing values. Current methods for imputation fail if the missing mechanism is not at random or if the level of missing exceeds 20% (23).

To identify significantly differentially expressed genes, statistical tests are commonly performed based on normalised intensity ratios (24; 25) or on estimated effects (9). Normal distributions cannot be assumed, so that bootstrap and permutation tests are used, requiring a relatively large number of replicates (5). Our method naturally describes dependencies and does not assume normality. Our ranking schemes and selection criteria are based on the joint distribution of concentrations or concentration ratios. Bayesian assessment of global significance can be easily implemented in our context (26). Dependencies between genes can be revealed from the joint distribution and graphically represented as a network (27). Since the main experimental factors are corrected for, estimated posterior dependencies can be interpreted as principally of biological origin.

Acknowledgement

We thank L. Holden, E. Hovig, M. Langaas, O. Myklebost, T. Stokke and B. Ylstra for discussions. Financial support was provided by The Norwegian Research Council, The Norwegian Microarray Consortium, The Norwegian Radium Hospital and The Norwegian Cancer Society.

References

1. Holloway, A, van Laar, R, Tothill, R, & Bowtell, D. (2002) *Nat. Genet. Suppl.* **32**, 481 – 489.

2. Butte, A. (2002) *Nat. Rev. Drug Discov.* **1**, 951–960.

3. Slonim, D. (2002) *Nat. Genet.* **32**, 502–508.

4. Churchill, G. (2002) *Nat. Genet.* **32**, 490–495.

5. Yang, Y & Speed, T. (2003) *Design and analysis of comparative microarray experiments*. (Chapman and Hall), pp. 35–92.

6. Townsend, J. (2003) *BMC Genomics* **4:41**.

7. Moreau, Y, Aerts, S, De Moor, B, De Stooper, B, & Dabrowski, M. (2003) *Trends Genet.* **19**, 570–577.

8. Quackenbush, J. (2002) *Nat. Genet.* **32**, 496–501.

9. Kerr, M, Martin, M, & Churchill, G. (2000) *J. Comput. Biol.* **7**, 819–837.

10. Newton, M, Kendziorsky, C, & Richmond, C. e. (2001) *J. Comp. Biol.* **8**, 37–52.

11. Nygaard, V, Løland, A, Holden, M, Langaas, M, Rue, H, Liu, F, Myklebost, O, Fodstad, Ø, Hovig, E, & Smith-Sørensen, B. (2003) *BMC Genomics* **4:11**.

12. Beaumont, M & Rannala, B. (2004) *Nat. Rev. Genet.* **5**, 251 – 261.

13. Peterson, A, Heaton, R, & Georgiadis, R. (2001) *Nucleic Acids Res.* **29**, 5163 – 5168.

14. Lyng, H, Badiee, A, Svendsrud, D. H, Hovig, E, Myklebost, O, & Stokke, T. (2004) *BMC Genomics* **5:10**.

15. Held, G, Grinstein, G, & Tu, Y. (2003) *Proc. Natl. Acad. Sci.* **100**, 7575–7580.

16. Dudley, A, Aach, J, Steffen, M. A, & Church, G. M. (2002) *Proc Natl Acad Sci USA* **99**, 7554–7559.

17. Hekstra, D, Taussig, A, Magnasco, M, & Naef, F. (2003) *Nucleic Acids Res.* **31**, 1962–1968.

18. Li, C & Wong, W. (2001) *Proc. Natl. Acad. Sci.* **98**, 31–36.

19. Townsend, J & Hartl, D. (2002) *Genome Biol.* **3**, research0071.1–0071.16.

20. Rhodes, D. R, Barrette, T. R, Rubin, M. A, Ghosh, D, & Chinnaiyan, A. M. (2002) *Cancer Res* **62**, 4427–4433.

21. Choi, J. K, Yu, U, Kim, S, & Yoo, O. J. (2003) *Bioinformatics* **19 Suppl. 1**, i84–i90.

22. Yang, Y, Dudoit, S, Luu, P, Lin, D. M, Peng, V, Ngai, J, & Speed, T. (2002) *Nucleic Acids Res* **30**.

23. Troyanskaya, O, Cantor, M, Sherlock, G, Brown, P, Hastie, T, Tibshirani, R, Botstein, D, & Altman, R. (2001) *Bioinformatics* **17**, 520–525.

24. Tusher, V, Tibshirani, R, & Chu, G. (2001) *Proc. Natl. Acad. Sci.* **98**, 5116–5121.

25. Pan, W. (2003) *Bioinformatics* **19**, 1333–1340.

26. Scott, J & Berger, J. O. (2004) An exploration of aspects of Bayesian multiple testing, (Duke University, www.isds.duke.edu/~berger/papers/multcomp.pdf), Technical Report 2003.

27. Troyanskaya, O, Dolinski, K, Owen, A. B, Altman, R. B, & Botstein, D. A. (2003) *Proc. Natl. Acad. Sci.* **100**, 8348 – 8353.

Figure Legends

Figure 1: Illustration of the microarray experiment. The various steps of the experiment and the corresponding covariates used in the model are listed with their symbols. The model consists of three levels: (i) selection, (ii) scanning and (iii) measurement.

In (i), K_g^1 and K_g^2 mRNA molecules for gene g present in sample 1 and 2 undergo a selection process. Each molecule succeeds or fails in each of the experimental steps: cDNA synthesis, dye labelling, purification, hybridisation and washing. Success for each molecule is modelled as a Bernoulli coin toss. The success probability depends on properties of the molecule and of the experiment (covariates). Molecules of the same gene can have different covariates, for example if they hybridise on different spots with different probes. If probe is in excess, molecules can be modelled as independent variables and the number of remaining molecules after each step is Binomially distributed. The probability of successfully passing through the entire experiment is the product of the probabilities of surviving each individual step. Nested Binomial variables are Binomial and the final number of molecules ready for being scanned is Binomial with two parameters: the unknown original number of transcripts per gene in each sample and the selection probability, modelled as in equation (2). Level (ii) describes the translation of the bound molecules remaining after washing ($H_s^{t,a}$, on array a, spot s, for sample $t = 1, 2$) into fluorescence intensities, as in equation (2). Measurement error (iii) of pixelwise intensities $L_{j,s}^{t,a}$ (on array a, pixel j on spot s for sample $t = 1, 2$) is assumed to be normally distributed as in equation (3). This model allows to obtain estimates of absolute concentrations K_g^1 and K_g^2 together with their posterior marginal probability density, as sketched at the bottom.

Figure 2: Validation of the methodology to estimate absolute numbers of transcripts. Control samples with 17 genes of known mRNA concentrations were used, each printed on six spots with six different pens. The inset in panel a shows the posterior probability density of the number of transcripts for a gene with estimated $5.8 \cdot 10^7$ mRNA molecules (mode) and its 95% credibility interval. There was lack of symmetry in the densities. Panel a and b show estimated numbers of mRNA molecules (y-axis) and true ones (x-axis) in $\log_{10}$-scale. Positions on the x-axis are slightly shifted to facilitate visualisation. Diagonal lines are shown; the fit is good when the line passes through the credibility interval. The data in panel A and B are based on two different dye-swap experiments. Analysis of the data in panel B, using the hybridisation factor from the data in panel A (0.001), showed a strong concordance between the two estimates, although the numbers of transcripts were slightly underestimated.

Figure 3: Comparison of the absolute transcript levels in a reference and a human cervical

tumour sample, estimated from two different experiments. The data in Table 1 were split into two sets of two arrays each and analysed separately, pretending no sample was shared. Estimated mRNA concentrations (number of mRNA molecules per μg of total RNA; posterior modes) are plotted for each gene and sample. Diagonal lines are shown. The two independently estimated concentrations Ref_1 and Ref_2 for the reference and B2_1 and B2_2 for sample $B2$ were similar and highly correlated. A small difference was observed for both samples, 0.188 in $\log_{10}$-scale for Ref and 0.231 for $B2$. This difference originated from the uncertainty in the estimation of β_0, a difficult task with just two arrays.

Figure 4: Probability of the four genes (see also Supporting Figure 9) to be among the n genes with the highest (red curve) or lowest (green curve) mRNA concentration (number of mRNA molecules per μg of total RNA). The plots clearly indicate if a gene is among those with high (gene 46), intermediate (genes 13 and 33) or low (gene 91) concentration.

Figure 5: Probabilities of genes to be among the 10 ones with the highest (red) and lowest (green) mRNA concentrations (number of mRNA molecules per μg of total RNA). See Supporting Table 2 for gene symbols. There are six genes with probability larger than 0.90 to have mRNA concentration among the 10 highest, and two genes to have concentrations among the 10 lowest ones. The value of the selection probability (here chosen as 0.90) should be as high as possible, but still such that enough genes are selected for the purpose of the study.

Figure 6: For a given group of genes, probability that all but m ratios of mRNA concentrations (number of mRNA molecules per μg of total RNA) in a human cervical tumour vs. reference are at least equal to k. The genes were ordered according to the probability that their ratio was among the ten highest, decreasingly. Gene 90 had highest probability. Up-regulated genes are indicated with "up", down-regulated with "do". We considered then all ordered subsets, following the given ranking: $\{90\}, \{90, 82\}, \{90, 82, 11\}$, and so on. For each such increasing subset of genes we computed the posterior probability that all but m ratios were at least k. Four curves are plotted, for various combinations of m and k. The more genes were included in the selected set, the smaller the probability became. The best set of genes with ratio at least two (k=2) and with at most one error (m=1) with 0.95 joint probability was the set $\{90, 82, 11, 14, 93, 25, 57, 34, 12, 60\}$. The larger the fold k and the smaller the accepted number of errors m, the more rapidly the probabilities decreased.

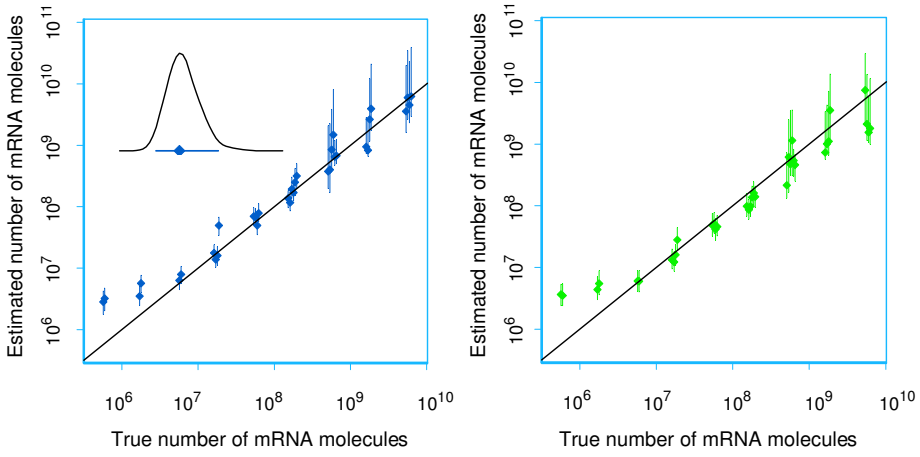
Estimated number of mRNA molecules
10^6
10^7
10^8
10^9
10^{10}
10^{11}
10^6
10^7
10^8
10^9
10^{10}
True number of mRNA molecules
Estimated number of mRNA molecules
10^6
10^7
10^8
10^9
10^{10}
10^{11}
10^6
10^7
10^8
10^9
10^{10}
True number of mRNA molecules

Figure 2

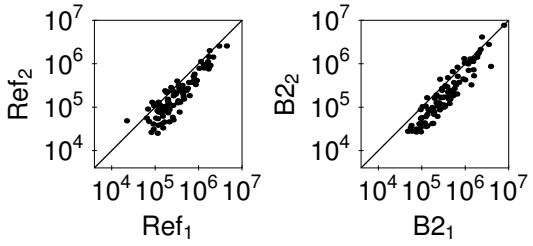
10^7
10^6
10^5
10^4
Ref_2
10^4 10^5 10^6 10^7
Ref_1
10^7
10^6
10^5
10^4
$B2_2$
10^4 10^5 10^6 10^7
$B2_1$

Figure 3

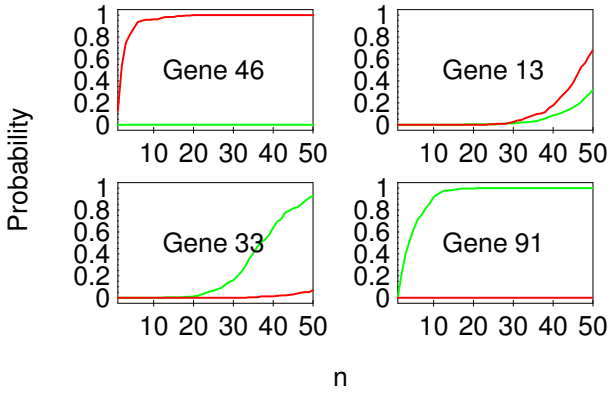
Probability
Gene 46
Gene 13
Gene 33
Gene 91
0
0.2
0.4
0.6
0.8
1
10 20 30 40 50
n

Figure 4

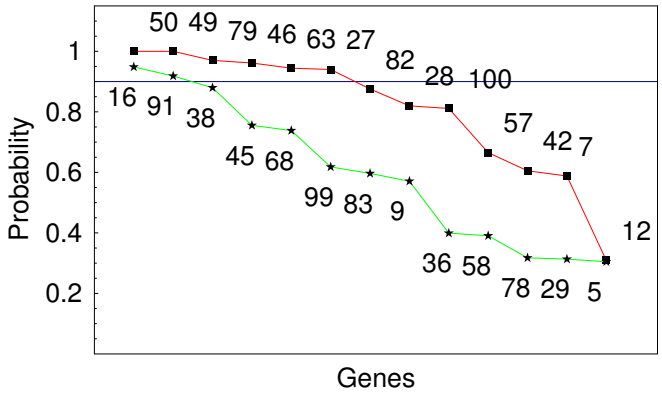
50 49 79 46 63 27 82 28 100 57 42 7 12
16 91 38 45 68 99 83 9 36 58 78 29 5
1
0.8
0.6
0.4
0.2
Probability
Genes

Figure 5

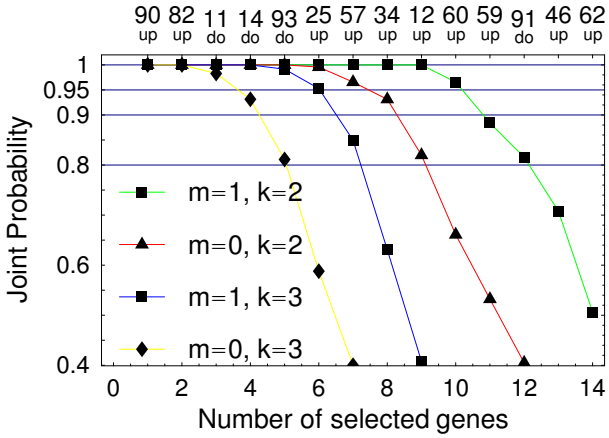
90 82 11 14 93 25 57 34 12 60 59 91 46 62
up up do do do up up up up up up do up up
1
0.95
0.9
0.8
0.6
0.4
Joint Probability
m=1, k=2
m=0, k=2
m=1, k=3
m=0, k=3
0
2
4
6
8
10
12
14
Number of selected genes

Figure 6

Model-based estimation of transcript concentrations from spotted microarray data.

Arnoldo Frigessi, Mark A. van de Wiel, Marit Holden, Ingrid K. Glad and Heidi Lyng

Supporting information

Supporting Methods

1 Model building

The experimental steps of the microarray experiment (Fig. 1 in the paper), seen from a statistical modelling point of view, are now discussed in turn.

cDNA synthesis and dye labelling.

Dye labelled cDNAs are achieved by incorporation of Cy3-dUTP and Cy5-dUTP during or after cDNA synthesis. The amount of dye and nucleotides are assumed to be in excess, so that all mRNA molecules can in principle be reverse transcribed and labelled. We assume that the expected number of actually bound Cy3- or Cy5-dUTP's is the same for all transcripts of all genes, since the number of binding sites, though different, is always large enough to allow for such a geometric approximation. The expected number of actually bound CyX-dUTP's does however depend on dye, i.e. there is a chemical dye effect. This effect will be important in the imaging step described below.

We assume the $q^{t,a} \cdot K_g^t$ molecules to be reverse transcribed and labelled independently of each other with probability $m_g^{t,a}$. Then, $M_g^{t,a}$, the resulting number of labelled cDNA molecules (or target molecules) for sample t, gene g and array a, follows the binomial distribution with parameters $q^{t,a} \cdot K_g^t$ and success probability $m_g^{t,a}$. The probability $m_g^{t,a}$ can depend on gene and sample specific covariates (like purity of the sample).

Purification.

The two samples are mixed. Excessive CyX-dUTP molecules are washed away. During this process also some of the target molecules will be lost. Let $V_g^{t,a}$ be the number of molecules, each independently remaining with probability $v_g^{t,a}$ in the solution after purification, for sample t, gene g and array a. Then $V_g^{t,a}$ is binomial with parameters $M_g^{t,a}$ and $v_g^{t,a}$. We expect that $v_g^{t,a}$ depends on the target sequence length of gene g, since target length possibly influences purification as longer molecules are less likely to be mistakenly washed away. After purification, the solution will still contain some remaining free CyX-dUTP's that will be washed away after hybridisation. Target length has not been included directly in the current model because target length information was not available. Differences in the $v_g^{t,a}$'s specifically caused by

target length will instead be absorbed in the gene specific covariate (β_g).

Hybridisation.

The variability of probe material and microarray production modulates the probability of successful hybridisation. For a certain spot the microarray, the pen and the probe used influence this probability. Consequently, both array and pen are included as covariates in the model, in addition to probe quantity and quality dependent covariates. Because each of the pens is used on a specific subgrid of the microarray, the pen effect may be confounded with spatial effects.

Quantity of the probe material may vary. A test slide of each printing batch is stained with SYBR green, a fluorophore with specific affinity for ssDNA, (1). The fluorescence intensity is used as an estimate of probe quantity of each spot of the arrays and is included as a covariate in the model. We do not distinguish here between spot center and periphery, assuming for simplicity that each part of a spot is equally covered by probe. Quality of the probe material may also vary. We distinguish two probe quality related covariates; the probe identification (PID) and the replication identification (RID). PID and RID distinguish genes replicated with equal or different probe sequence. PID accounts specifically for the effect of different probes, and RID for replications of equal probe.

We assume that the target is homogeneous, i.e. the spatial distribution of each target molecule is uniform over the slide and target molecules do not cluster nor repulse. Let gene(s) be the gene spotted in spot s. A proportion $c \cdot n_s^a$ of $V^{t,a}_{\text{gene}(s)}$ reaches the correct spot to candidate for hybridisation. Let $Q_s^{t,a}$ be the number of gene(s) molecules of sample t succeeding in hybridising to spot s, in array a. Each target molecule has a probability $q_s^{t,a}$ to independently hybridise. Then $Q_s^{t,a}$ is binomial with parameters $c \cdot n_s^a \cdot V^{t,a}_{\text{gene}(s)}$ and $q_s^{t,a}$. The success probability $q_s^{t,a}$ depends on probe properties and technical experimental conditions as well as on target properties. The first two classes include probe quantity, probe length, PID, RID, pen and array. Target length influences the diffusion coefficient of target molecules and could have been included here also, if available. Hybridisation is assumed to be dye independent (2) and the hybridisation probability is assumed to be constant in time. The model does not include cross-hybridisation.

Washing.

We assume that all non-hybridised material, including unbound CyX-dUTPs, is removed during microarray washing. Again we assume that the number of remaining molecules $H_s^{t,a}$ is binomial with parameters $Q_s^{t,a}$ and success probability $h_s^{t,a}$, which may depend on probe length, reflecting the binding strength, and on microarray effects. $H_s^{t,a}$ is the number of gene(s) molecules of sample t hybridised in spot s in array a, participating in the imaging process.

Scanning and image analysis.

The image achieved during scanning is gridded and segmented into spots. Each measured pixel intensity, $L_{j,s}^{t,a}$, for sample t, array a and pixel j of spot s depends on $H_s^{t,a}$, on the PMT voltage used during scanning and on a known scanner dependent amplification factor. In addition the measured intensity depends on whether sample t was labelled with Cy3- and Cy5-dUTP's. This dye dependency has both chemical and optical reasons. As described previously, the expected number of actually bound CyX-dUTP's might be different for Cy3-

or Cy5-dUTP's, i.e. there is a chemical dye effect. The optical dye effect is present because of different optical characteristics of the two dyes.

The model.

Nesting all bionomial variables results in the bionomial model presented in the paper. The success probabilities depend on covariates from all the steps mentioned above. All effects are estimated together with the unknown K_g^t's and $H_s^{t,a}$'s.

2 Reparametrisation of the model, identifiability, constraints and hyper-priors

Recall the four levels of our model:

$$\begin{aligned}
H_s^{t,a} &\sim \text{Binomial}(c \cdot n_s^a \cdot q^{t,a} \cdot K_g^t, p_s^{t,a}),\\
p_s^{t,a} &= \max[1, \exp\{\beta_0 + \beta_e + \beta_a + \beta_p + \beta_g + \beta_{\text{RID}} + \beta_{\text{PID}}\\
&\quad + \beta_l \cdot [\text{probe length}] + \beta_q \cdot [\text{probe quantity}] + \beta_m \cdot [\text{purity}_t]\}],\\
\mu_s^{t,a} &= 2^{f_{\text{dye}}\,\text{PMT}^{t,a}} H_s^{t,a} \alpha_{\text{dye}},\\
L_{j,s}^{t,a} &= \frac{\mu_s^{t,a}}{n_s^a} + \varepsilon_{j,s}^{t,a}, \quad \varepsilon_{j,s}^{t,a} \sim \text{Normal}(0, (\sigma_s^{t,a})^2).
\end{aligned}$$

Introduce

$$\bar{\beta} X_s^a = \beta_a + \beta_p + \beta_{\text{RID}} + \beta_{\text{PID}} + \beta_l \cdot [\text{probe length}] + \beta_q \cdot [\text{probe quantity}],$$

so that

$$p_s^{t,a} = \max[1, \exp\{\beta_0 + \beta_e + \beta_g + \beta_m \cdot [\text{purity}_t] + \bar{\beta} X_s^a\}].$$

In a classical likelihood context all parameters must be identifiable, while in the Bayesian setting flat posterior densities correspond to model misspecification or lack of information in the data on parameters. MCMC convergence is then particularly slow. We require classical identifiability of the parameters and discuss now how the parameters can be estimated within our framework. We will show identifiability under the relaxed inverse link function $\exp(x)$ instead of $\max(1, \exp(x))$, which is used in practice, and assuming all parameters are fixed. This is allowed, because the censored inverse link function that we use and non-flat priors on the fixed effects (which is the Bayesian way of introducing a random effect) only restrict the size of the parameter space.

For computational purposes, it is useful to approximate binomials with normal densities:

$$H_s^{t,a} \sim \text{Normal}\big(c \cdot n_s^a \cdot q^{t,a} \cdot K_g^t \cdot p_s^{t,a}, c \cdot n_s^a \cdot q^{t,a} \cdot K_g^t \cdot p_s^{t,a} \cdot (1 - p_s^{t,a})\big).$$

Next, we reparameterise in such a way that parameters not estimable based on the mean alone do not occur in the mean, but only in the variance. We have

$$E[L_{j,s}^{t,a}] = E[\mu_s^{t,a}]/n_s^a = C^{t,a} \cdot K_g^t \cdot \alpha_{\text{dye}} \exp(\beta_0 + \beta_e + \beta_g + \beta_m \cdot [\text{purity}_t]) \exp(\bar{\beta} X_s^a),$$

where $C^{t,a}$ is a product of known constants. Then, let

$$\alpha_{\text{dye}} = \alpha'_{\text{dye}} \alpha$$

where $\alpha'_{\text{Cy5}} = 1$, and α'_{Cy3} and α are the new parameters to be estimated, replacing α_{Cy3} and α_{Cy5}. In addition $\tilde{H}$'s and $\tilde{K}$'s replace the H's and K's, where the $\tilde{H}$'s and $\tilde{K}$'s are defined as follows

$$\tilde{H}_s^{t,a} = H_s^{t,a} \cdot \alpha$$

$$\tilde{K}_g^t = K_g^t \cdot \alpha \, \exp(\beta_0 + \beta_e + \beta_g + \beta_m \cdot [\text{purity}_t]).$$

Then, we observe that

$$\tilde{H}_s^{t,a} \sim \text{Normal}\Big(c \cdot n_s^a \cdot q^{t,a} \cdot \tilde{K}_g^t \cdot \exp(\bar{\beta} X_s^a), \\ c \cdot n_s^a \cdot q^{t,a} \cdot \tilde{K}_g^t \exp(\bar{\beta} X_s^a)\big(1 - \exp(\beta_0 + \beta_e + \beta_g + \beta_m \cdot [\text{purity}_t] + \bar{\beta} X_s^a)\big) \cdot \alpha \Big).$$

Since $E[L_{j,s}^{t,a}] = C^{t,a} \cdot \tilde{K}_g^t \alpha'_{\text{dye}} \exp(\bar{\beta} X_s^a)$, all parameters except β_0, β_e, β_m, the β_g's and α are estimable based on the mean pixel-wise values with the described reparametrisation, when the regression of this mean on the covariates X_s^a is identifiable. This can be guaranteed by some constratints (see below) and with a design which has the following characteritics: some genes must be spotted at least in duplicate, with different pens for some of these replicates, and the whole data set must include at least one loop, i.e. a self-self array or a dye swap or a longer chain, to identify the parameters α'_{dye}, β_a and β_p.

The parameters β_0, β_e, β_m, α and the β_g are estimable from the variances and none of these occur in the expressions for the mean. Some care is required to handle the special situation of samples hybridised only once on one array. This happens for example in reference designed studies. Since there is just one piece of data relative to such samples for non-repeated genes, these data must be excluded when inference on variance related parameters is perfomed, since otherwise estimated uncertainties of the concentrations will be shrinked. We operate as follows: First we exclude all such single data points and estimate all parameters on the rest of the data. In a reference design, this corresponds to using all data of the reference and all data from the samples for repeated genes. We then use the posterior distribution of all parameters as prior in the second phase, where we consider only the rest of the data, those corresponding to samples and genes measured only ones. We thus obtain the correct estimates for all concentrations, equipped with the coherently propagated uncertainty. In practice, all is performed within MCMC: sampled values from the posterior distribution of all parameters given the repeatedly observed samples are used in the model for the uniquely observed data. This second phase is not necessary in loop designs or when dye swaps are included. Finally, transcript concentration K_g^t is estimated using the estimates of $\tilde{K}_g^t$, β_0, β_e, β_m, α and β_g by inverting the formula above.

We need to constrain the categorical parameters for identifiability. In order to assure identifiability of the pen parameters, we use the constraint $\sum \beta_p = 0$, where the summation runs over the P different values β_p may attain, when P different pens are used. A similar constraint is used for the parameter β_e describing the effect of different non-transitive experiments and the gene related parameters β_g (to ensure identifiability together with β_0). For each set of experiments e, $\sum \beta_a = 0$, where the sum runs over all arrays of the transitive set e. Moreover, we restrict the mean effect of all probes per gene to be zero which is achieved by applying the constraints $\sum \beta_{PID} = 0$, for all genes, where summation runs over all probes in the probe set of the particular gene. Similarly, we constrain $\sum \beta_{RID} = 0$, for all probes, where summation runs

over all replicates for the particular probe. In addition to these constraints we consider experiment (β_e), array (β_a), pen (β_p), gene-dependent selection (β_g), probe identification (β_{PID}) and replication identification (β_{RID}) as random effects. Then, we have $\beta_e \sim \text{Normal}(0, (\sigma_e)^2)$, $\beta_a \sim \text{Normal}(0, (\sigma_a)^2)$, $\beta_p \sim \text{Normal}(0, (\sigma_p)^2)$ and $\beta_g \sim \text{Normal}(0, (\sigma_g)^2)$. Since the number of probe products per gene is usually small, we do not use separate random effects for each gene, but instead we have $\beta_{\text{PID}} \sim \text{Normal}(0, (\sigma_{\text{PID}})^2)$ for all probe sequences. Similarly, we have $\beta_{\text{RID}} \sim \text{Normal}(0, (\sigma_{\text{RID}})^2)$ for all replications of probe. Otherwise, all hyper-parameters are equipped with flat improper non-informative priors.

The identifiability of all parameters, including the transcript concentrations K_g^t, assures that two experiments that both satisfy the identifiability conditions above can be combined, *even* when they do not share a sample and hence non-transitive designs are allowed.

On the link function We have discussed reparametrisation and identifiability under the inverse link $\exp(x)$. Within an MCMC context this can easily be adapted to a censored inverse link by not accepting proposals for which $\exp(\beta_0+\beta_e+\beta_g+\beta_m\cdot[\text{purity}_t]+\bar{\beta}X_s^a) > 1$. One might be inclined to use the proportional, non-censored inverse link instead of the censored inverse link. However, use of the censored inverse link conserves the complicated non-proportional effects of factors. We know that these exist in the original formulation with an intercept, because mapping a linear combination of factors to a number between 0 and 1 implies non-proportionality.

Overdispersion The covariates in the model should explain the selection probability as good as possible. However, some explanatory factors might be missing from the model. Moreover, individual molecules may not have completely identical selection probabilities due to differences on a molecular level. We can allow for overdispersion by adding variability to the selection probability using a spot, array and sample varying random model error $\epsilon_s^{t,a}$ with distribution $\text{Normal}(0, \sigma^2)$. We note, however, that estimation of σ^2 together with the other variance related parameters may lead to slow convergence of the MCMC. In the human cervical tumour study we included overdispersion in order to confirm that identifiability is maintained also in this case. In the validation example no overdispersion was included.

Competition We have not included competition among molecules in our model for hybridisation. This is possible to do in terms of density dependence, for example by adding the term $\beta K^t_{\text{gene}(s)}$ in the log-probability. Then, we expect β to be negative: the larger $K^t_{\text{gene}(s)}$, the more competition and hence the smaller the probability to hybridise.

Other Bayesesian microarray studies For more examples of Bayesian inference for statistical models of gene expression data we refer to Baldi and Hatfield (3) and references therein. None of these deal with absolute concentrations.

3 Initial values and proposal functions: Details on MCMC

The marginal posteriors of interest are not available in closed form and so we use Markov Chain Monte Carlo to sample from the posterior model. Specifically, we implement a single-

update random-walk Metropolis-Hastings sampler. Convergence is difficult to monitor (4) and we used very long chains, started after burn-in with different random seeds, and observed convergence to the same posterior parameter densities. A block-updating strategy might improve convergence. For all the model parameters we use a uniform proposal. More precisely, let v be the current value of the parameter p for which a new value will be proposed, and let $c_{p,0}$ and $c_{p,1}$ be two constants. If the parameter is not restricted to be positive, draw from

$$U[v - c_{p,1}\sigma_p, v + c_{p,1}\sigma_p]$$

if the prior for the parameter is Normal$(0, \sigma_p^2)$, otherwise draw from

$$U[v - (c_{p,1}|v| + c_{p,0}), v + (c_{p,1}|v| + c_{p,0})].$$

If the parameter is restricted to be positive, draw the logarithm of the parameter from

$$U[log(v) - (c_{p,1}log(v) + c_{p,0}), log(v) + (c_{p,1}log(v) + c_{p,0})].$$

The two constants for each parameter p, $c_{p,0}$ and $c_{p,1}$, were tuned such that reasonable acceptance rates were obtained, between 0.2 and 0.5. After reparametrisation the parameters to be estimated are α'_{Cy3}, α, the β's, the overdispersion ε's, σ, variances of the random effects, the $\tilde{H}$'s and the $\tilde{K}$'s. Initial parameter estimates for α'_{Cy3}, the β's (except for β_0, β_m, the β_e's and the β_g's), the overdispersion ε's and σ are found from the data using linear regression. The variances of the random effects, the $\tilde{H}$'s and the $\tilde{K}$'s are then computed from these estimates. In the computations of all these initial estimates we use formulas where all random variables are set equal to their expectations. The parameters $\beta_0, \beta_m, \beta_e$'s and the β_g's are initialised such that for each gene g, the geometric mean of the selection probabilities $p_s^{t,a}$ becomes 0.5. Finally, α is set equal to the geometric mean of

$$(\tilde{H}_s^{t,a} - c \cdot n_s^a \cdot q^{t,a} \cdot \tilde{K}_g^t \cdot \exp(\bar{\beta} X_s^a))^2 / (c \cdot n_s^a \cdot q^{t,a} \cdot \tilde{K}_g^t \cdot \exp(\bar{\beta} X_s^a) \cdot (1 - p_s^{t,a})).$$

Details on the MCMC, such as the number of iterations, are available here:

http://www.nr.no/pages/samba/area_emr_smbi_transcount.

References

1. Battaglia, C., Salani, G., Bernardi, L. R., and De Bellis G. Analysis of DNA microarrays by non-destructive fluorescent staining using SYBR green II. *Biotechniques* 29, 78 - 81 (2000).

2. Wang, Y., Wang, X, Guo, S.-W. and Ghosh, S. Conditions to ensure competitive hybridization in two-color microarray: a theoretical and experimental analysis. *Biotechniques* 32, 1342 - 1346 (2002).

3. Baldi, P. and Hatfield, G.W. *DNA microarrays and gene expression - From experiments to data analysis and modeling.* Cambridge University Press (2002).

4. Frigessi, A., Martinelli, F. and Stander, J. Computational complexity of Markov Chain Monte Carlo methods for finite Markov Random Fields. *Biometrika* 84, 1 - 18 (1997).

Supporting Materials

Array Slides. cDNA microarray slides were produced at the cDNA Microarray Facility at The Norwegian Radium Hospital (http://www.mikromatrise.no). The probes were human cDNA clones, derived from the I.M.A.G.E. Consortium (http://image.llnl.gov) or locally prepared, amplified by PCR and printed to Corning CMT GAPS slides (Corning) by using a Microgrid II printing robot (BioRobotics) with 32 pens. Each array contained 18432 spots printed in 32 subarrays. Some probes were printed in duplicate with different pens, and some probes with different cDNA sequence representing the same genes. Probe length ranged from 525 to over 2000 base pairs; in this latter case, 2000 was used as covariate value in our models. Furthermore, for validation of our method, seventeen DNA control samples (Lucidea Universal ScoreCard, Amersham Biosciences) were printed in equal amount on six of the subarrays.

Sample Preparation and Hybridisation. Validation was performed adding two control samples, each containing 17 different mRNA sequences, pre-mixed at specific concentrations (Lucidea Universal ScoreCard). 0.5 μl of each sample was used, corresponding to a number of transcripts in the range of $5.8 \times 10^5 - 5.8 \times 10^9$. The concentration ratios achieved when hybridising the two samples together were 1:1, 1:3, 3:1, 1:10, and 10:1 at high and low level concentrations. The control samples were prepared as described by the manufacturer and subjected to cDNA synthesis and dye labelling as described below. The labelled samples were hybridized together in a dye-swap design. Hybridisation was performed overnight at 65^oC by use of Genetac hybridisation station (Perkin Elmer).

Furthermore, two tumour biopsies (A, B) and a reference sample (Ref) of total RNA (Stratagene) were used. The reference sample was pooled from ten human cell lines. The biopsies, $(5\ \text{mm})^3$ in size, were from two different locations in a human cervical tumour. Biopsy B was divided into two pieces (B1, B2) before isolation of total RNA. Total RNA was isolated from the biopsies using Trizol reagent (Invitrogen) and the recommended protocol. Fifty to sixty μg of total RNA were used to produce labelled cDNA by anchored oligo(dT)-primed reverse transcription, using SuperScript II reverse transcriptase (Invitrogen) and either Cy3-dUTP or Cy5-dUTP (Amersham Pharmacia). The labeled samples were hybridized in a loop design overnight in water bath at 65^oC (Table 1). Purity was optimal and equal for all samples in our experiments and was therefore not used in our models.

Scanning and Image Analysis. The slides were imaged at a resolution of 10 μm using an Agilent G2565BA scanner (Agilent Technologies) for slides with control samples and a ScanArray4000 scanner (GSI Lumonics) for slides with biopsies and reference. A laser power of 100% was used. The PMT voltage was adjusted for the red and green channel individually to ensure that the intensity of the weakest spots and background segments were within the linear range of the scanner. Saturated spot intensities were corrected using the algorithm described previously in Lyng et al (2004)(reference (15) in the paper). The GenePix 3.0 image analysis software (Axon Instruments) was used for spot segmentation and intensity calculation. Bad spots and regions with high unspecific binding of dye were manually flagged and excluded from the analysis.

Supporting Table 2: Parameter estimates

We considered 100 genes in 158 spots of each array. Totally, there are 127 β_{PID}'s, since 27 genes were duplicated with different probe sequence. Because of the contraints put on the β_{PID}'s 73 of these are set to zero. The other 54 are divided into pairs which are constrained such that the sum of the β_{PID}'s for each pair is zero. In the table the estimate for one β_{PID} from each of the 27 pairs is given. Similarly, there are 158 β_{RID}'s, since 58 genes were duplicated either with different (27) or with equal (31) probe sequence. Because of the contraints put on the β_{RID}'s 96 of these are set to zero. The other 62 are divided into pairs which are constrained such that the sum of the β_{RID}'s for each pair is zero. In the table the estimate for one β_{RID} from each of the 31 pairs is given. In the paper the probe length effect was discussed. We see that it is in the same scale as the array effect and hence contributes similarly to the selection probability. The probe lengths have been scaled to zero mean and standard deviation one, making the β's comparable. β_m has not been included in the model because purity was optimal and equal for all samples. There is no experiment effect, $\beta_e = 0$, since this experiment was transitive.

Parameter	Mode	95% Credibility Interval	Parameter	Mode	95% Credibility Interval	Parameter	Mode	95% Credibility Interval
β_0	-2.343	(2.614, -2.074)	β_g, 47	0.002	(-0.301, 0.341)	β_{PID}, 6	-0.149	(-0.48, 0.143)
α	1.589	(1.195, 2.102)	48	0.004	(-0.345, 0.322)	7	-1.604	(-1.938, -1.226)
α'_{Cy3}	0.365	(0.355, 0.383)	49	0.01	(-0.352, 0.336)	8	0.199	(-0.262, 0.629)
β_l	-0.17	(-0.335, 0.036)	50	-0.01	(-0.32, 0.287)	9	-0.266	(-0.614, 0.169)
β_q	0.254	(0.106, 0.431)	51	-0.009	(-0.167, 0.617)	10	0.172	(-0.07, 0.481)
β_a,1	-0.535	(-0.585, -0.481)	52	-0.024	(-0.353, 0.266)	11	0.141	(-0.214, 0.517)
2	-0.041	(-0.086, 0.005)	53	-0.017	(-0.333, 0.359)	12	0.222	(-0.081, 0.596)
3	0.178	(0.133, 0.227)	54	0.022	(-0.321, 0.326)	13	0.216	(-0.084, 0.623)
4	0.396	(0.347, 0.44)	55	0.014	(-0.346, 0.339)	14	0.206	(-0.083, 0.525)
β_p,1	0.011	(-0.066, 0.342)	56	-0.007	(-0.316, 0.321)	15	0.061	(-0.335, 0.414)
2	0.001	(-0.124, 0.309)	57	0.022	(-0.351, 0.316)	16	1.155	(0.789, 1.633)
3	0.001	(-0.253, 0.111)	58	0.003	(-0.281, 0.315)	17	-0.086	(-0.363, 0.27)
4	-0.018	(-0.354, 0.037)	59	0.011	(-0.302, 0.283)	18	-1.366	(-1.607, -1.096)
5	-0.003	(-0.152, 0.128)	60	-0.01	(-0.316, 0.354)	19	0.45	(0.133, 0.763)
β_g,1	-0.012	(-0.374, 0.251)	61	0	(-0.288, 0.337)	20	0.45	(0.177, 0.676)
2	0.003	(-0.295, 0.337)	62	0.022	(-0.305, 0.327)	21	0.159	(-0.253, 0.479)
3	0.013	(-0.363, 0.288)	63	0.015	(-0.293, 0.299)	22	-0.559	(-0.885, -0.195)
4	-0.017	(-0.362, 0.316)	64	0.011	(-0.288, 0.327)	23	-0.475	(-0.817, -0.128)
5	-0.018	(-0.33, 0.385)	65	0.015	(-0.325, 0.35)	24	-0.395	(-0.734, -0.076)
6	-0.03	(-0.35, 0.34)	66	-0.005	(-0.37, 0.36)	25	1.267	(0.958, 1.618)
7	0.011	(-0.35, 0.333)	67	0	(-0.39, 0.284)	26	0.041	(-0.256, 0.351)
8	0.016	(-0.382, 0.327)	68	-0.007	(-0.344, 0.296)	27	-0.233	(-0.544, 0.069)
9	0.008	(-0.363, 0.333)	69	0.008	(-0.326, 0.36)	β_{RID}, 1	0.09	(-0.189, 0.348)
10	0.017	(-0.357, 0.327)	70	-0.011	(-0.335, 0.374)	2	0.379	(0.087, 0.676)
11	-0.002	(-0.342, 0.333)	71	0.018	(-0.338, 0.401)	3	-0.127	(-0.364, 0.172)
12	-0.003	(-0.352, 0.302)	72	-0.01	(-0.552, 0.083)	4	0.136	(-0.171, 0.408)
13	-0.009	(-0.36, 0.329)	73	0.016	(-0.367, 0.233)	5	0.199	(-0.054, 0.472)
14	0.003	(-0.315, 0.384)	74	-0.006	(-0.366, 0.3)	6	-0.522	(-0.82, -0.152)
15	-0.016	(-0.309, 0.294)	75	0.008	(-0.295, 0.238)	7	0.569	(0.134, 0.881)
16	-0.014	(-0.319, 0.368)	76	0.028	(-0.391, 0.34)	8	-1.19	(-1.515, -0.75)
17	-0.003	(-0.441, 0.286)	77	0.022	(-0.31, 0.348)	9	0.109	(-0.144, 0.387)
18	0.01	(-0.325, 0.374)	78	0.002	(-0.355, 0.275)	10	-0.356	(-0.72, 0.039)
19	-0.007	(-0.319, 0.354)	79	-0.005	(-0.391, 0.274)	11	-1.022	(-1.342, -0.715)
20	-0.003	(-0.361, 0.252)	80	0.008	(-0.322, 0.34)	12	-0.62	(-0.964, -0.333)
21	-0.024	(-0.344, 0.316)	81	-0.001	(-0.356, 0.385)	13	-0.093	(-0.447, 0.241)
22	-0.011	(-0.36, 0.313)	82	0.003	(-0.376, 0.289)	14	-1.334	(-1.643, -0.978)
23	-0.009	(-0.295, 0.376)	83	-0.013	(-0.33, 0.334)	15	-0.007	(-0.329, 0.368)
24	0.02	(-0.326, 0.331)	84	0.021	(-0.337, 0.354)	16	-0.057	(-0.305, 0.303)
25	-0.004	(-0.134, 0.397)	85	-0.016	(-0.337, 0.319)	17	1.277	(1.036, 1.6)
26	0.014	(-0.308, 0.354)	86	-0.004	(-0.283, 0.353)	18	0.432	(0.13, 0.83)
27	0.014	(-0.315, 0.339)	87	0.026	(-0.358, 0.29)	19	0.462	(0.191, 0.846)
28	-0.019	(-0.354, 0.329)	88	0.015	(-0.356, 0.327)	20	-0.515	(-0.78, -0.087)
29	-0.017	(-0.336, 0.341)	89	0.015	(-0.353, 0.304)	21	0.493	(0.242, 0.765)
30	-0.007	(-0.317, 0.296)	90	0.013	(-0.317, 0.324)	22	0.177	(-0.06, 0.48)
31	0.011	(-0.308, 0.325)	91	-0.014	(-0.375, 0.302)	23	-0.086	(-0.429, 0.181)
32	0.007	(-0.303, 0.371)	92	0.004	(-0.304, 0.233)	24	0.192	(-0.051, 0.526)
33	0.003	(-0.301, 0.356)	93	0.022	(-0.319, 0.358)	25	0.037	(-0.307, 0.319)
34	-0.004	(-0.136, 0.482)	94	0.001	(-0.27, 0.366)	26	0.161	(-0.135, 0.461)
35	-0.015	(-0.352, 0.308)	95	-0.01	(-0.351, 0.369)	27	-0.459	(-0.737, -0.123)
36	-0.019	(-0.311, 0.311)	96	-0.023	(-0.396, 0.317)	28	0.286	(0.06, 0.592)
37	0.017	(-0.339, 0.313)	97	0.003	(-0.342, 0.382)	29	-0.154	(-0.563, 0.214)
38	0.017	(-0.314, 0.314)	98	0.023	(-0.327, 0.321)	30	0.352	(0.024, 0.622)
39	0	(-0.278, 0.253)	99	-0.007	(-0.359, 0.296)	31	0.179	(-0.123, 0.501)
40	-0.019	(-0.324, 0.34)	100	0.02	(-0.262, 0.348)	σ_{PID}	0.599	(0.53, 0.702)
41	-0.018	(-0.3, 0.291)	β_{PID}, 1	-0.057	(-0.321, 0.333)	σ_{RID}	0.556	(0.485, 0.61)
42	-0.003	(-0.318, 0.373)	2	0.06	(-0.201, 0.323)	σ_p	0.041	(0.011, 0.346)
43	-0.002	(-0.32, 0.325)	3	0.057	(-0.186, 0.275)	σ_a	0.34	(0.2, 1.031)
44	-0.002	(-0.292, 0.363)	4	0.011	(-0.307, 0.418)	σ_g	0.034	(0.011, 0.365)
45	0.009	(-0.354, 0.311)	5	0.561	(0.301, 0.855)	σ	0.294	(0.269, 0.321)
46	-0.005	(-0.354, 0.318)						

Supporting Table 3: Correlations between estimated concentrations in the second experiment

In the second experiment, four arrays were hybridised in a loop design with three samples (A, B1, B2) from a human cervical tumour and a reference sample (Ref) (Table 1).

Estimated concentrations for individual genes were reliable, as pairwise scatterplots (Supporting Figure 8), and correlations in the following table show.

Supporting Table 3: Correlation between estimated concentrations

	Sample B1	Sample B2	Sample A
Ref	0.258	0.280	0.396
A	0.912	0.928	
B2	0.993		

These relationships were consistent with A, B1 and B2 originating from the same tumour and B1 and B2 originating from the same location within the tumour.

Supporting Table 4: Estimates of absolute transcript concentrations

For the human cervical tumour study we considered 100 genes and four samples; reference, biopsy B1, biopsy B2 and biopsy A. The estimated number of transcripts for each gene in each sample is given together with its uncertainty. The estimates are posterior marginal modes and the uncertainties are described by 95% credibility intervals, lying between the 2.5% and the 97.5% quantiles.

Gene Number and name		Reference Mode and 95% credibility interval ($*10^6$)		Biopsy B1 Mode and 95% credibility interval ($*10^6$)		Biopsy B2 Mode and 95% credibility interval ($*10^6$)		Biopsy A Mode and 95% credibility interval ($*10^6$)	
1	*ABR*	0.308	(0.18, 0.718)	0.406	(0.227, 0.862)	0.385	(0.225, 0.858)	0.543	(0.293, 1.122)
2	*ARPC2*	0.132	(0.063, 0.258)	0.151	(0.082, 0.338)	0.2	(0.112, 0.417)	0.181	(0.098, 0.357)
3	*B4GALT1*	0.318	(0.145, 0.634)	0.213	(0.118, 0.492)	0.243	(0.118, 0.489)	0.263	(0.125, 0.498)
4	*BCL2A1*	0.059	(0.031, 0.174)	0.077	(0.03, 0.174)	0.092	(0.053, 0.264)	0.127	(0.057, 0.257)
5	*CAPZB*	0.095	(0.044, 0.236)	0.093	(0.046, 0.266)	0.087	(0.044, 0.231)	0.085	(0.039, 0.187)
6	*CASP3*	0.426	(0.176, 1.019)	0.925	(0.393, 2.056)	0.615	(0.282, 1.621)	0.544	(0.265, 1.449)
7	*CASP7*	1.209	(0.695, 3.054)	1.314	(0.739, 2.884)	1.295	(0.767, 3.33)	1.585	(0.96, 3.691)
8	*CCT6A*	1.01	(0.511, 1.887)	0.741	(0.399, 1.497)	1.06	(0.578, 2.229)	1.248	(0.644, 2.227)
9	*CD34*	0.055	(0.024, 0.157)	0.055	(0.026, 0.18)	0.064	(0.03, 0.169)	0.092	(0.042, 0.239)
10	*CD37*	0.098	(0.051, 0.33)	0.16	(0.079, 0.468)	0.177	(0.09, 0.528)	0.184	(0.092, 0.54)
11	*CD44*	3.531	(2.087, 8.298)	0.513	(0.306, 1.255)	0.711	(0.332, 1.428)	1.716	(0.82, 3.614)
12	*CD53*	0.401	(0.25, 0.977)	0.926	(0.489, 1.837)	1.151	(0.718, 2.729)	1.801	(0.999, 3.757)
13	*CDC6*	0.528	(0.284, 1.14)	0.289	(0.14, 0.616)	0.279	(0.16, 0.599)	0.329	(0.182, 0.712)
14	*CDH13*	0.561	(0.326, 1.23)	0.112	(0.064, 0.279)	0.1	(0.063, 0.251)	0.238	(0.122, 0.501)
15	*CDK8*	0.403	(0.247, 0.905)	0.498	(0.274, 0.944)	0.557	(0.295, 1.003)	0.465	(0.288, 1.008)
16	*CDK9*	0.06	(0.026, 0.144)	0.043	(0.018, 0.126)	0.047	(0.024, 0.134)	0.045	(0.023, 0.131)
17	*CDKN1B*	0.269	(0.125, 0.676)	0.453	(0.22, 1.058)	0.337	(0.189, 0.907)	0.412	(0.208, 0.957)
18	*CDKN2D*	0.243	(0.132, 0.603)	0.262	(0.135, 0.574)	0.289	(0.146, 0.601)	0.297	(0.173, 0.778)
19	*CHL1*	0.112	(0.067, 0.366)	0.159	(0.085, 0.541)	0.208	(0.112, 0.634)	0.299	(0.171, 0.779)
20	*CKS2*	0.984	(0.511, 1.838)	0.41	(0.227, 0.819)	0.583	(0.357, 1.301)	0.99	(0.565, 2.116)
21	*CLCN3*	0.324	(0.154, 0.736)	0.323	(0.159, 0.797)	0.297	(0.133, 0.579)	0.235	(0.106, 0.466)
22	*CLDN3*	0.106	(0.046, 0.278)	0.096	(0.048, 0.311)	0.113	(0.049, 0.287)	0.062	(0.032, 0.192)
23	*CLIC1*	0.081	(0.043, 0.186)	0.178	(0.092, 0.407)	0.177	(0.103, 0.431)	0.158	(0.076, 0.309)
24	*COL15A1*	0.176	(0.098, 0.384)	0.139	(0.07, 0.285)	0.131	(0.076, 0.306)	0.252	(0.148, 0.592)
25	*COL1A2*	0.26	(0.159, 0.537)	0.933	(0.56, 1.839)	0.73	(0.491, 1.479)	1.123	(0.71, 1.928)
26	*COX10*	0.172	(0.079, 0.424)	0.124	(0.053, 0.306)	0.142	(0.073, 0.355)	0.135	(0.072, 0.347)
27	*COX7C*	1.553	(0.864, 3.878)	1.823	(0.976, 4.194)	2.098	(1.075, 4.548)	1.85	(1.037, 4.788)
28	*CREG*	1.151	(0.615, 2.17)	1.733	(0.98, 3.674)	1.793	(0.894, 3.555)	1.389	(0.828, 3.171)
29	*CSK*	0.087	(0.046, 0.186)	0.114	(0.059, 0.249)	0.091	(0.05, 0.204)	0.079	(0.041, 0.166)
30	*CYP2A7*	0.216	(0.124, 0.473)	0.34	(0.186, 0.694)	0.319	(0.172, 0.626)	0.246	(0.111, 0.412)
31	*DDX16*	0.239	(0.142, 0.561)	0.373	(0.196, 0.754)	0.352	(0.216, 0.785)	0.425	(0.198, 0.737)
32	*DUSP5*	0.133	(0.065, 0.274)	0.156	(0.086, 0.359)	0.155	(0.094, 0.364)	0.096	(0.052, 0.226)
33	*EPHA1*	0.157	(0.076, 0.34)	0.187	(0.097, 0.405)	0.219	(0.105, 0.44)	0.206	(0.117, 0.497)
34	*ETS2*	0.186	(0.114, 0.407)	0.782	(0.459, 1.508)	0.674	(0.345, 1.131)	0.622	(0.345, 1.117)
35	*FLJ00023*	0.305	(0.185, 0.67)	0.333	(0.188, 0.661)	0.384	(0.229, 0.788)	0.555	(0.287, 1.002)
36	*FLJ10701*	0.063	(0.029, 0.161)	0.072	(0.033, 0.186)	0.082	(0.043, 0.217)	0.087	(0.043, 0.206)
37	*FLJ10871*	0.342	(0.16, 0.856)	0.594	(0.288, 1.535)	0.463	(0.255, 1.192)	0.288	(0.159, 0.788)
38	*FN1*	0.137	(0.064, 0.284)	0.048	(0.026, 0.129)	0.06	(0.027, 0.137)	0.077	(0.041, 0.172)
39	*FNTA*	0.227	(0.145, 0.467)	0.244	(0.191, 0.596)	0.413	(0.23, 0.758)	0.387	(0.273, 0.728)
40	*FY*	0.099	(0.049, 0.21)	0.12	(0.074, 0.296)	0.121	(0.061, 0.256)	0.09	(0.053, 0.211)
41	*GADD34*	0.203	(0.115, 0.514)	0.127	(0.066, 0.351)	0.21	(0.106, 0.496)	0.223	(0.123, 0.546)
42	*GAPD*	2.253	(1.296, 5.399)	1.31	(0.62, 2.75)	1.599	(0.81, 3.246)	1.89	(1.052, 4.546)
43	*GPM6B*	0.129	(0.08, 0.28)	0.092	(0.05, 0.218)	0.088	(0.049, 0.203)	0.091	(0.047, 0.177)
44	*GSTA2*	0.112	(0.057, 0.32)	0.173	(0.085, 0.446)	0.116	(0.054, 0.281)	0.109	(0.046, 0.235)
45	*GSTA3*	0.084	(0.043, 0.216)	0.066	(0.034, 0.211)	0.065	(0.034, 0.2)	0.049	(0.021, 0.114)
46	*GSTP1*	1.036	(0.496, 2.789)	2.727	(1.234, 6.845)	2.915	(1.292, 6.885)	2.103	(1.098, 5.482)
47	*GSTTLp28*	0.56	(0.318, 1.245)	0.665	(0.348, 1.495)	0.604	(0.403, 1.557)	0.763	(0.421, 1.621)
48	*HDGF*	1.12	(0.564, 2.156)	1.405	(0.702, 2.633)	1.242	(0.659, 2.4)	0.888	(0.521, 2.117)
49	*HLA-C*	0.528	(0.267, 1.506)	9.238	(3.8, 20.511)	8.572	(4.233, 20.923)	6.456	(2.641, 14.813)
50	*HLA-DPB1*	0.101	(0.053, 0.255)	3.127	(1.635, 6.909)	3.754	(1.909, 7.065)	4.908	(3.17, 12.066)

Continued on next page

Gene Number and name		Reference Mode and 95% credibility interval ($*10^6$)		Biopsy B1 Mode and 95% credibility interval ($*10^6$)		Biopsy B2 Mode and 95% credibility interval ($*10^6$)		Biopsy A Mode and 95% credibility interval ($*10^6$)	
51	*HXB*	0.667	(0.396, 1.45)	0.38	(0.229, 0.92)	0.398	(0.212, 0.798)	0.888	(0.594, 2.227)
52	*IGF1*	0.142	(0.065, 0.343)	0.379	(0.156, 0.787)	0.32	(0.141, 0.654)	0.297	(0.139, 0.657)
53	*IGF1R*	0.291	(0.138, 0.678)	0.142	(0.064, 0.345)	0.145	(0.08, 0.419)	0.151	(0.073, 0.338)
54	*IGHG3*	0.138	(0.076, 0.336)	0.187	(0.107, 0.504)	0.204	(0.104, 0.436)	0.184	(0.101, 0.433)
55	*IL10RA*	0.122	(0.059, 0.315)	0.233	(0.121, 0.542)	0.24	(0.131, 0.608)	0.223	(0.105, 0.509)
56	*IL13RA1*	0.189	(0.117, 0.582)	0.305	(0.159, 0.844)	0.309	(0.148, 0.833)	0.217	(0.114, 0.621)
57	*IL1R2*	0.508	(0.22, 1.082)	2.374	(1.05, 4.696)	1.607	(0.71, 3.429)	1.212	(0.63, 2.811)
58	*IL1RN*	0.093	(0.045, 0.258)	0.09	(0.045, 0.29)	0.08	(0.043, 0.263)	0.075	(0.034, 0.189)
59	*IL6*	0.113	(0.054, 0.279)	0.331	(0.178, 0.698)	0.263	(0.147, 0.6)	0.249	(0.136, 0.541)
60	*IL8*	0.088	(0.038, 0.232)	0.194	(0.097, 0.525)	0.219	(0.106, 0.517)	0.413	(0.203, 0.955)
61	*IRF1*	0.149	(0.088, 0.365)	0.2	(0.116, 0.491)	0.16	(0.105, 0.426)	0.213	(0.106, 0.39)
62	*JUN*	0.146	(0.066, 0.349)	0.232	(0.12, 0.6)	0.283	(0.142, 0.686)	0.451	(0.232, 1.106)
63	*JUNB*	0.538	(0.295, 1.256)	2.297	(1.181, 4.826)	1.823	(1.149, 4.443)	1.432	(0.848, 3.214)
64	*KIAA1705*	0.211	(0.112, 0.461)	0.1	(0.055, 0.244)	0.108	(0.061, 0.277)	0.147	(0.077, 0.308)
65	*KLF2*	0.117	(0.065, 0.262)	0.138	(0.076, 0.317)	0.105	(0.061, 0.249)	0.105	(0.06, 0.241)
66	*LAMB1*	0.414	(0.225, 0.812)	0.251	(0.149, 0.574)	0.324	(0.187, 0.665)	0.402	(0.22, 0.747)
67	*LMNA*	0.465	(0.283, 0.987)	0.388	(0.22, 0.823)	0.461	(0.248, 0.896)	0.427	(0.29, 1.015)
68	*LOX*	0.094	(0.048, 0.233)	0.045	(0.024, 0.125)	0.057	(0.03, 0.145)	0.125	(0.069, 0.311)
69	*MAPK14*	0.379	(0.193, 0.904)	0.425	(0.204, 1.015)	0.372	(0.214, 1.028)	0.768	(0.399, 1.946)
70	*MCAM*	2.323	(1.392, 5.289)	0.51	(0.304, 1.214)	0.598	(0.332, 1.245)	0.76	(0.448, 1.74)
71	*MEG3*	0.195	(0.108, 0.443)	0.195	(0.102, 0.387)	0.188	(0.114, 0.392)	0.176	(0.111, 0.42)
72	*MID1*	0.109	(0.064, 0.298)	0.398	(0.211, 0.872)	0.376	(0.276, 0.985)	0.507	(0.293, 1.109)
73	*MY014*	0.224	(0.116, 0.456)	0.166	(0.071, 0.29)	0.135	(0.076, 0.296)	0.169	(0.085, 0.322)
74	*NGFB*	0.206	(0.104, 0.464)	0.195	(0.093, 0.423)	0.134	(0.066, 0.292)	0.087	(0.044, 0.219)
75	*OAZ1*	0.987	(0.704, 2.485)	1.026	(0.652, 2.35)	1.049	(0.721, 2.517)	1.188	(0.731, 2.354)
76	*ODC1*	3.129	(1.763, 6.841)	0.566	(0.346, 1.249)	0.552	(0.365, 1.388)	0.803	(0.537, 2.061)
77	*OSTF1*	0.436	(0.259, 0.949)	0.603	(0.33, 1.228)	0.37	(0.241, 0.881)	0.382	(0.215, 0.76)
78	*PAPPA*	0.112	(0.067, 0.263)	0.071	(0.039, 0.18)	0.061	(0.04, 0.172)	0.119	(0.07, 0.256)
79	*PC4*	1.628	(0.964, 3.631)	1.704	(1.07, 4.083)	2.195	(1.219, 4.627)	2.183	(1.301, 5.453)
80	*PFKM*	0.302	(0.177, 0.649)	0.163	(0.083, 0.305)	0.142	(0.09, 0.327)	0.182	(0.098, 0.329)
81	*PIM1*	0.205	(0.087, 0.494)	0.19	(0.086, 0.504)	0.189	(0.107, 0.599)	0.318	(0.129, 0.62)
82	*PLAU*	0.232	(0.116, 0.59)	2.35	(1.04, 4.531)	1.878	(1.01, 4.523)	1.458	(0.74, 3.349)
83	*PLGL*	0.07	(0.031, 0.151)	0.087	(0.047, 0.209)	0.084	(0.035, 0.175)	0.063	(0.028, 0.126)
84	*PPP2R1B*	0.374	(0.218, 0.752)	0.183	(0.098, 0.392)	0.2	(0.101, 0.373)	0.208	(0.129, 0.477)
85	*PSMC4*	1.397	(0.873, 2.823)	1.263	(0.742, 2.677)	1.238	(0.643, 2.277)	1.249	(0.791, 2.628)
86	*PTE1*	0.302	(0.178, 0.606)	0.184	(0.106, 0.448)	0.18	(0.119, 0.447)	0.167	(0.097, 0.331)
87	*RAB6A*	1.014	(0.514, 1.836)	0.59	(0.298, 1.067)	0.48	(0.269, 0.915)	1.159	(0.666, 2.261)
88	*RAF1*	0.274	(0.153, 0.653)	0.242	(0.124, 0.518)	0.268	(0.145, 0.62)	0.548	(0.295, 1.137)
89	*RI58*	0.103	(0.047, 0.248)	0.261	(0.119, 0.506)	0.251	(0.128, 0.576)	0.247	(0.122, 0.581)
90	*S100A7*	0.047	(0.022, 0.155)	0.679	(0.361, 1.511)	1.035	(0.628, 2.846)	0.255	(0.135, 0.635)
91	*SERPINA1*	0.128	(0.058, 0.323)	0.052	(0.023, 0.163)	0.046	(0.02, 0.13)	0.045	(0.028, 0.149)
92	*SFRS9*	0.561	(0.361, 1.224)	0.361	(0.228, 0.814)	0.441	(0.249, 0.929)	0.622	(0.315, 1.112)
93	*SLC2A3*	0.332	(0.2, 0.812)	0.094	(0.05, 0.23)	0.085	(0.049, 0.202)	0.088	(0.044, 0.2)
94	*TM4SF3*	0.407	(0.271, 0.924)	0.465	(0.318, 1.053)	0.5	(0.302, 1.018)	0.579	(0.336, 1.127)
95	*TP53BP1*	0.418	(0.252, 0.915)	0.269	(0.127, 0.515)	0.241	(0.156, 0.594)	0.348	(0.192, 0.656)
96	*TRIP7*	0.531	(0.318, 1.122)	0.804	(0.44, 1.633)	1.038	(0.576, 2.014)	0.934	(0.522, 1.998)
97	*TSC2*	0.214	(0.106, 0.443)	0.163	(0.085, 0.37)	0.109	(0.075, 0.285)	0.129	(0.068, 0.274)
98	*UFD1L*	0.153	(0.081, 0.37)	0.165	(0.081, 0.381)	0.171	(0.088, 0.383)	0.133	(0.08, 0.341)
99	*VDR*	0.123	(0.064, 0.26)	0.081	(0.041, 0.177)	0.052	(0.028, 0.127)	0.078	(0.042, 0.171)
100	*VEGF*	1.172	(0.699, 3.381)	1.794	(0.983, 5.296)	1.91	(1.025, 5.029)	1.703	(1.008, 4.766)

Supporting Figure 7: validation of the methods: Estimated ratios between numbers of molecules per gene in two samples with known concentrations

Estimated ratios between numbers of molecules per gene in the two samples were obtained. The data in Figure 7 are based on the dye-swap experiment presented in Figure 2a in the paper. Estimated ratios of the numbers of mRNA molecules of the two samples are plotted for each of the 17 genes, together with their 95% credibility intervals. Horizontal lines represent true ratios, coloured squares are estimated ratios with a colour for each true ratio. Nine genes have true ratio 1. True ratios 10, 3, 1, 0.33 and 0.10 are coloured yellow, green, pink, red and blue respectively. The ratios are sufficiently well estimated; for example, when the true fold is 1, estimates range between 1 and 1.5. One 10-fold is estimated however as a 3-fold. A two- or three-fold cut-off analysis would correctly deliver 4 overexpressed and 4 underexpressed genes. Estimated ratios of number of molecules were similar to the ratios of normalised measured intensities; in both cases folds were sufficiently well estimated to guide a search for differential expressions.

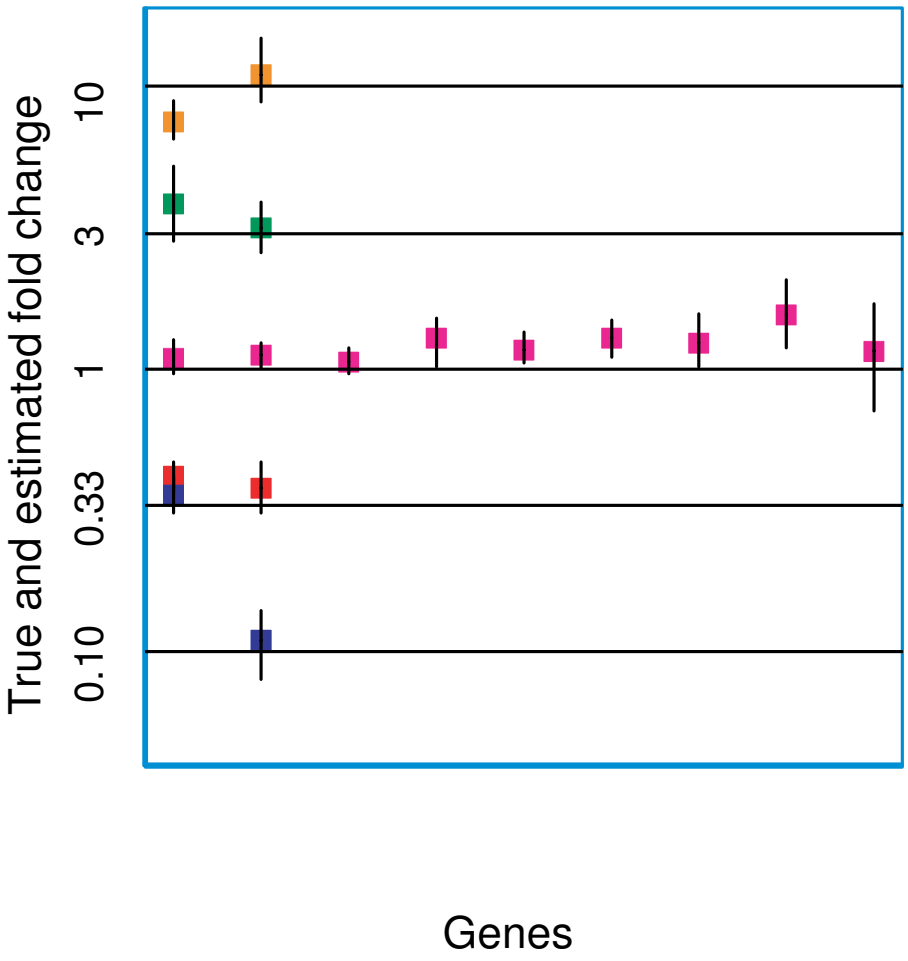
True and estimated fold change
10
3
1
0.33
0.10
Genes

Supporting Figure 8: Comparison of absolute transcript levels in different samples from a human cervical tumour

Comparison of absolute transcript levels in different samples from a human cervical tumour. The data are based on the experiments listed in Table 1 in the paper. Estimated mRNA concentrations (number of mRNA molecules per μg of total RNA; posterior modes) are plotted for each gene and sample. Correlation coefficients and diagonal lines are shown. The remaining two correlation coefficients are 0.280 for reference versus sample B2 and 0.396 for reference versus sample A. The estimated mRNA concentrations for the tumour samples (A, B1, B2) showed a much stronger correlation to each other than to the reference sample (Ref). Moreover, the two samples derived from the same biopsy (B1, B2) were more correlated to each other than to the sample derived from a different location in the tumour (A). Notice that the range obtained by multiplying estimated concentrations in the biopsies by the quantity of total RNA leads to estimated numbers of transcripts, which are within a range comparable to that of the validation experiment in Figure 2a and 2b in the paper.

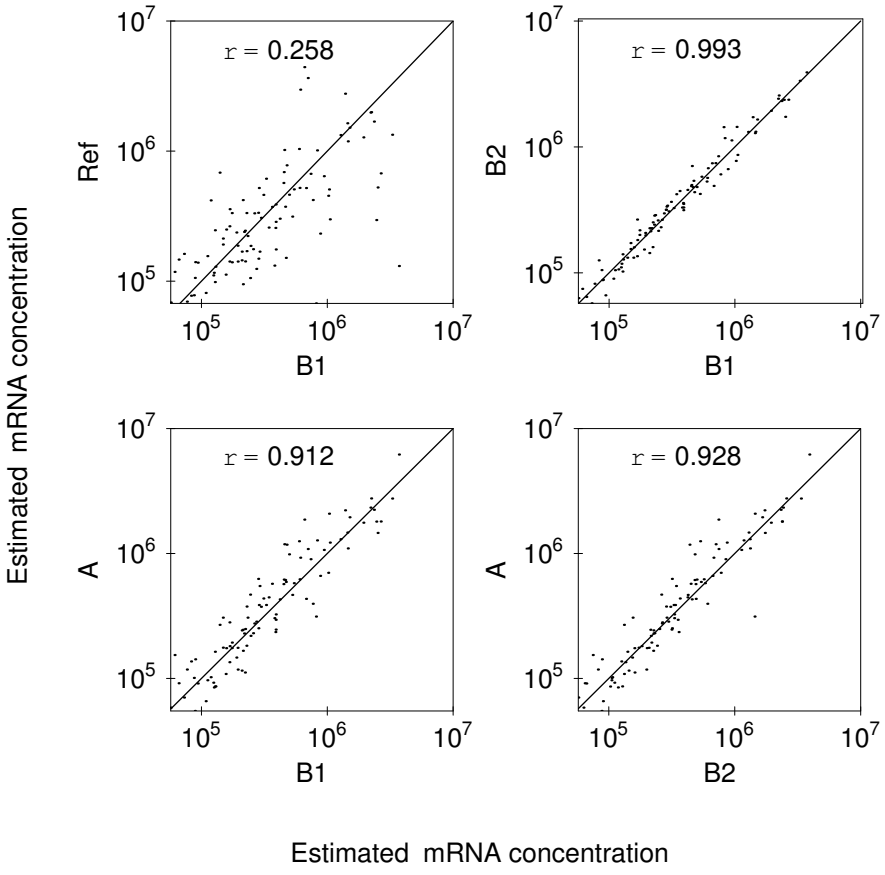

Supporting Figure 9: Estimated probability densities of mRNA concentration in samples from a human cervical tumour

Estimated probability densities of mRNA concentration (number of mRNA molecules per μg of total RNA) in a cervical tumour for four typical genes; gene 13, 33, 46, and 91 (see Supporting Table 2 for the gene symbols of the 100 genes included in the analysis). The data are based on the experiments listed in Table 1, and represent the distributions of the mean concentrations of the three tumour samples (A, B1, B2). The width of the credibility intervals describe the biological variability of the three samples in addition to the uncertainty of the estimates. Gene 46 had a relatively high mRNA concentration, gene 91 low, while the other two were intermediate. Different axis scales are used for the different genes.

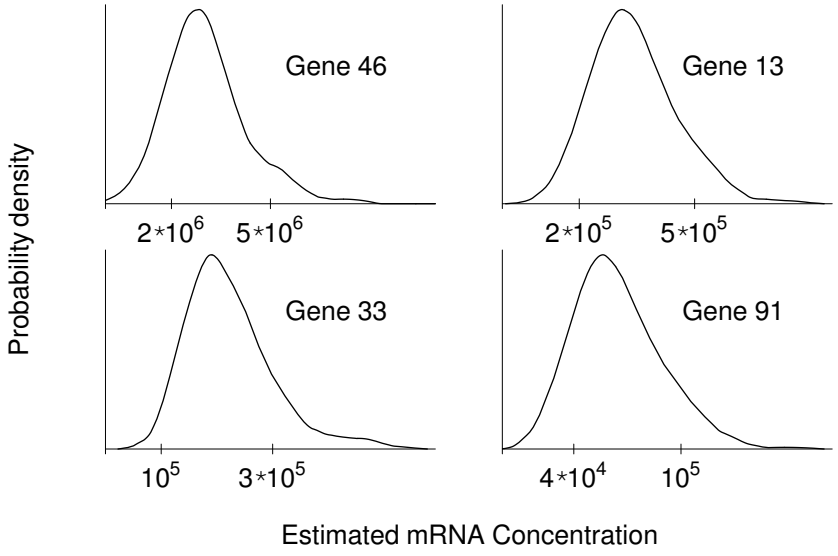

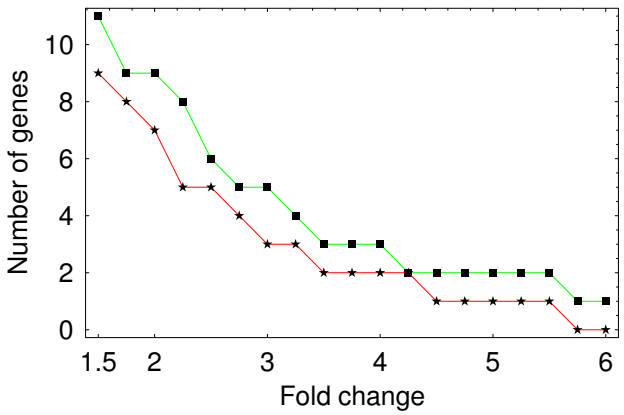

Figure 1:

Supporting Figure 10: the number of selected genes as function of the fold k

We plotted the number of selected genes as a function of the fold k, for a given value of the probability that all but m genes were at least k-fold expressed. We used $m = 0$ and two values of the probability, 0.95 (red) and 0.80 (green), for the two curves. This plot helps to find the required balance between level of differential expression (here the fold k) and the number of selected genes, for a given level of posterior probability.